RECENT RESULTS FROM NA44

Daniel S. Zachary
E-mail: zachary@vxcern.cern.ch
Ohio State University, Columbus, OH 433212, USA

(for the NA44 COLLABORATION)

Abstract

The NA44 experiment at CERN has measured single particle spectra and two-particle correlations in Pb + Pb collisions. Comparisons are made to p + Pb, S + S, and S + Pb reactions and an analysis of the transverse mass distributions of pions, kaons and protons are discussed. An increased proton inverse slope is seen in lead reactions when compared to the slopes found in sulfur reactions. Proton rapidity densities are also shown for central Pb + Pb collisions and a large degree of nuclear stopping is observed. Two-particle interferometry has also been preformed for pions and kaons. Correlation measurements in Pb + Pb collisions show that the source size for both pions and kaons is larger than the source size measured in S + S and S + Pb reactions.

1 The NA44 Experiment

The NA44 focusing spectrometer is used to measure particles originating from proton (450 A·GeV/c), sulfur (200 A·GeV/c) and lead (158 A·GeV/c) beams incident on various targets. The spectrometer covers a transverse momentum range of $0 \leq p_t \leq 1.5$ GeV/c, obtained by taking data at two angular settings, 44 and 131 mrad with respect to the beam axis.

The front half of the spectrometer consists of two warm dipoles and three superconducting quadrupoles. Particles emitted from the target are focused to a plane approximately 10 meters downstream. For the data shown in this paper, the operating momentum range is ±20 % around the nominal values of 4 and 8 GeV/c.

The interaction and centrality trigger is provided via two scintillators located downstream from the target, covering the range $1.5 < \eta < 3.3$. A silicon multiplicity pad detector is also located just downstream from the target and is used offline for event characterization. Event triggering requires at least one hit detected by each of the hodoscopes. For A + A collisions, a central event is defined as the most central 8.7 ± 2.0 % of σ_{geom} in S + S and S + Pb reactions and $6.4 \pm 1.5\%$ of σ_{geom} in Pb + Pb reactions.

Particle identification is performed via two Cherenkov tanks and three hodoscope counters (for TOF measurements). The timing resolution for the scintillator hodoscope is $\sigma_{TOF} < 100$ps giving a momentum resolution of $\delta p/p \approx 0.2$ %. The start timing signal for the TOF measurement is produced via a Cherenkov beam counter located 60cm in front of the target with a resolution of $\approx$ 35 ps. For all particle species, particle contamination is less than 5%.

A uranium-scintillator calorimeter (UCAL) allows identification of e's and μ's. Other tracking chambers have been added for the 1994 and 1995 lead running period, including two strip chambers and a Multi-Particle Threshold Imaging Cherenkov (TIC)[1]. Full details of the NA44 spectrometer can be found in [2].

2 Single Particles

The goal of relativistic heavy-ion collisions is to create a hot, dense hadronic matter in the laboratory and to see a transition to a deconfined quark-gluon-plasma (QGP) phase. Single particle momentum spectra provide a means to study these collisions and a means to search for signatures of the QGP phase of matter. Lead beams at CERN provide the heaviest collisions at the highest energy produced to date for accelerators. Collective effects such as rescattering, thermodynamic behavior, and flow, are expected to be the greatest for the largest systems. Nuclear stopping is also expected to be greater for these large collision systems and experimentally it has already been found that nuclear stopping in light-ion S + S collisions is greater than that found in p + p collisions [3].

The yield dN/m$_t$dm$_t$ for pions, kaons and protons is shown in Fig. 1 for S + S and Pb + Pb collisions. This quantity is plotted as a function of transverse kinetic energy m$_t$ - m, where m$_t$ = $\sqrt{p_t\ +\ m_o}$, and m_o is m$_p$, m$_k$, or m$_\pi$. Data are plotted from two momentum settings, 4 and 8 GeV/c. The solid line represents a fit of a single exponential of the form f(m$_t$,T) = A $\cdot$ e$^{-m_t/T}$. The data has been corrected for geometrical acceptance, momentum resolution, reconstruction efficiency and decays in flight [4]. This fit does reasonable well except for pions at low momentum. The contribution to the pion cross-section above the exponential fit is attributed mostly from decaying η's, ω's, and ρ's[4].

The values next to each curve represent the inverse slope and in parenthesis is the statistical error. Larger inverse slope parameters for heavier particles is found and inverse slopes increase preferentially for heavier particles as the collision system is increased. This phenomena has been predicted by Landau [5] and has been attributed to transverse flow [6].

The rapidity distribution for protons has been measured near midrapidity (2 $\leq$ y $\leq$ 3). The results are plotted in Fig. 2. The errors shown are statistical only and the systematic errors are estimated to be 26.8% and 32.7% for data from the 4 and 8 GeV/c settings respectively. The data is compared with the models RQMD[7] and FRITIOF[8]. The Pb + Pb proton data supports a large proton rapidity density around midrapidity and hence a large degree of nuclear stopping. This data is in contrast with p + p and S + S collisions where relatively little proton rapidity density is observed at midrapidity [9]. The FRITIOF calculations, predicting a dip in the proton rapidity distribution, disagrees with the measured result. The FRITIOF model allows for no secondary rescattering and therefore very little stopping is expected. Although there is a large degree of stopping observed, the data disagrees with the RQMD prediction of a proton peak at midrapidity. Proton rapidity densities observed at midrapidity are in agreement with results from experiment NA49[10].

The large amount of nuclear stopping at midrapidity suggests a high degree of hadronic rescattering and therefore a comparison to thermodynamic models is suggested. A recent thermodynamic model by Schnedermann et al [6], includes a simple model for radial flow. The mass spectrum for this model is describe by the integral,

$$\frac{dN}{m_t dm_t} \propto \int_0^R r dr m_t I_o \left(\frac{p_t sinh(\rho)}{T_{fo}} \right) K_1 \left(\frac{p_T cosh(\rho)}{T_{fo}} \right), \tag{1}$$

where $\rho = \tanh^{-1}\beta_r$, $\beta_r(r) = \beta_s(r/R)^\alpha$, and $\alpha = 1$ for these calculations. The functions I$_o$ and K$_1$

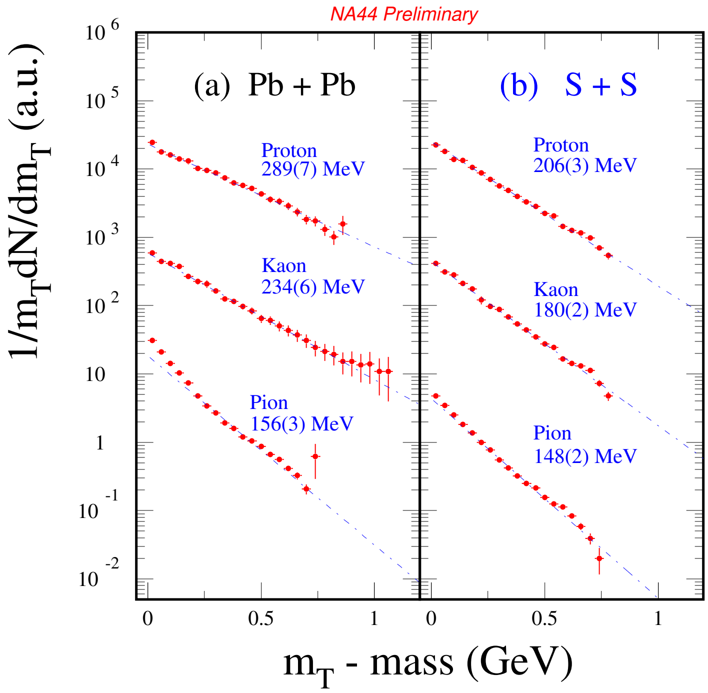

Figure 1: PRELIMINARY momentum spectra (arbitrary units) for p, K^+, and π^+ for S + S and Pb + Pb collisions. The solid lines are exponential fits to the data, A$\cdot$ e $^{-m_t/T}$.

are modified Bessel functions. This model has been applied to all three particle simultaneously for both collisions systems of Fig. 1. The extracted parameters are T_{fo} = 140 MeV, β_s = 0.41 (radial velocity) for S + S collisions and T_{fo} = 140 MeV, β_s = 0.6 for Pb + Pb collisions. One should note that these values represent a suggested combination of T_{fo} and β_s.

3 Two-Particle Correlation Measurements

Two-particle correlations provides information of the space-time extent of the emission source. Originally this technique was developed by Hanbury-Brown, and Twiss (HBT) and was used to measure the angular extent of stars [11] and has since been applied to heavy-ion collisions. One possible signature for the quark-gluon plasma is an extended emission time for mesons from a system undergoing a phase change [12], [13], [14].

Operationally, the correlation function is constructed by taking the ratio of the two-particle cross-section $R(\vec{k_1},\vec{k_2})$, and the product of the single particle cross-sections, $B(\vec{k_1},\vec{k_2})$ [4].

$$C_{raw}(\vec{k_1},\vec{k_2}) \;=\; \frac{R(\vec{k_1},\vec{k_2})}{B(\vec{k_1},\vec{k_2})}, \qquad (2)$$

where k_i are particle momenta.

The data is compared with a theoretical curve which is constructed from a Fourier transform of the spatial density distribution of the emission source, $\rho = e^{-r^2/2R^2}$. In this model, the source is assumed to be chaotic with no spatial-momentum correlations. Furthermore, no particle interactions are assumed to occur after the particles "freezeout". Various corrections to the raw correlation function are applied [4], including Gamow corrections for Coulomb interactions. Another correction is needed for the distortion of the single particle background due to Bose-Einstein correlations among particles in the narrow NA44 acceptance. Finally, a correction must be included for the geometrical acceptance of the experiment.

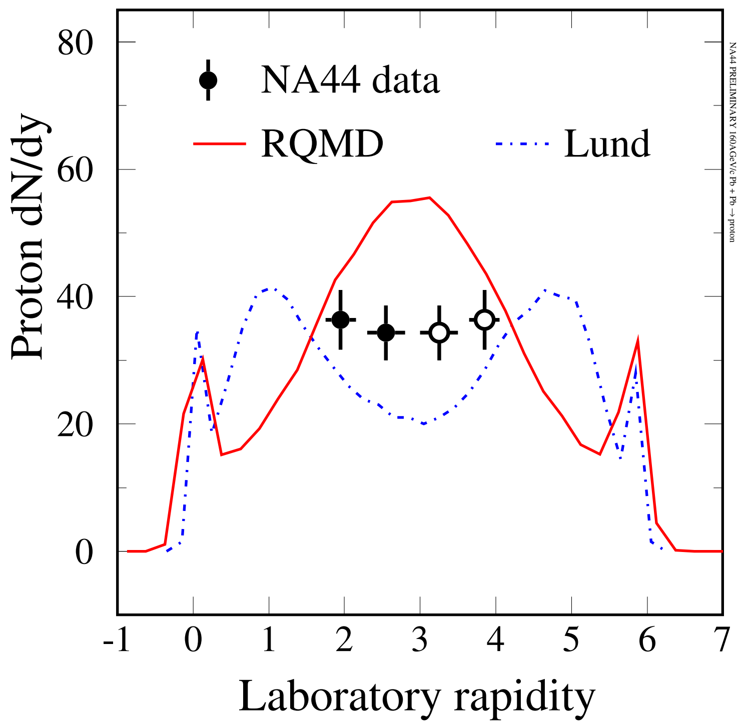

Figure 2: PRELIMINARY dN/dy distribution for protons in central (upper 6.7% of σ_{geom}) Pb + Pb collisions. Open points represent data reflected about midrapidity (y = 2.9). Comparisons are made to the transport models RQMD and FRITIOF. The RQMD calculations includes decays from λ's and other resonance baryons. At midrapidity 67 $\pm$ 9 % of the protons originating from λ decay are accepted into the NA44 spectrometer.

Our statistics permit an analysis of the correlation function in one and three dimensions for p + Pb, S + S, S + Pb and Pb + Pb collisions.

$$C(Q_{inv}) \;=\; A(1 \;+\; \lambda e^{-Q_{inv}^2 R^2}) \tag{3}$$

$$C(Q_{TO}, Q_{TS}, Q_L) \;=\; A(1 \;+\; \lambda e^{-Q_{TO}^2 R_{TO}^2 - Q_{TS}^2 R_{TS}^2 - Q_L^2 R_L^2}), \tag{4}$$

where Q_{inv} is the invariant momentum difference in one dimension and Q_{TO}, Q_{TS}, and Q_L are the invariant momentum differences in the transverse-out (parallel to the pair-momentum sum), transverse-side (perpendicular to the pair-momentum sum), and longitudinal directions. The data are analyzed in the frame in which the longitudinal component of the momentum is zero, ie., (p_{z1} + p_{z2}) = 0. The results of the $\pi^+\pi^+$ correlation function along with the fitted curve in one and three dimensions are shown in Fig. 3.

Fig. 4 shows a comparisons of $\pi^+\pi^+$ and K^+K^+ radii and chaoticity parameters for p + Pb, S + Pb, and Pb + Pb reactions. Results show that $R_L \approx R_{TS} \approx R_{TO}$. Both kaon and pion radii increase with the size of the collision system. Correlation radii for pions are systematically larger than those for kaons and this suggests that kaons originate from a more central region of the collision. Secondly, decaying η's, ω's and ρ's play a role in enlarging the measured freezout radius for pions. One technique to distinguish this contribution is to perform measurements in the high momentum setting (where $<p_t> \approx$ 450 MeV/c) and compare results to measurements from a low momentum setting (where $<p_t> \approx$ 150 MeV/c). The two data clusters representing S + Pb collisions in Fig. 4 show this difference.

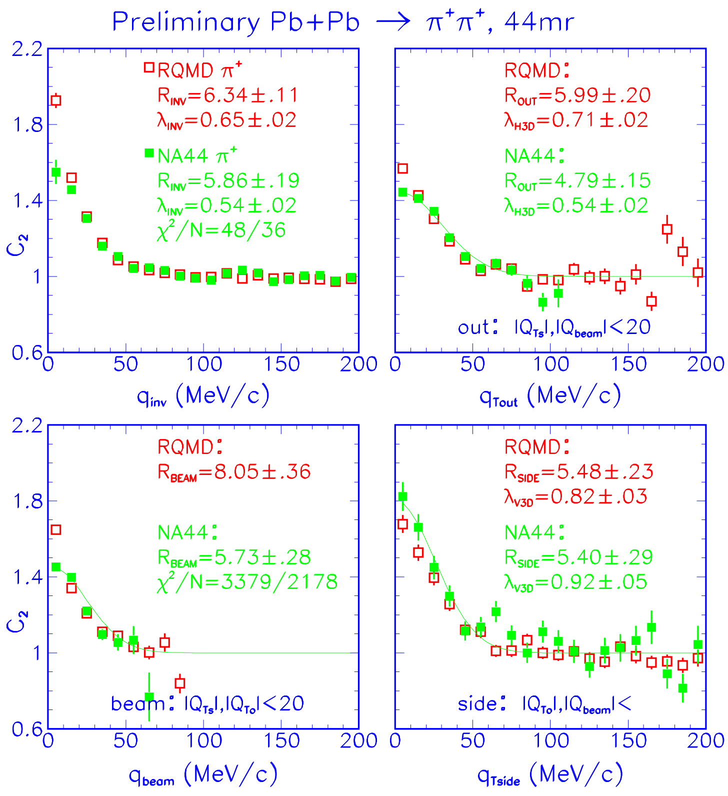

Figure 3: PRELIMINARY results of the correlation function for a one and three dimensional analysis of $\pi^+\pi^+$ in Pb + Pb collisions. Fitted parameters are also plotted for RQMD calculations.

4 Conclusions

Single particle spectra and two-particle correlations have been measured in p + A and A + A collisions at CERN. The single particle spectra for p, K^+, and π^+ are well described by the function $C{\cdot}e^{-m_t/T}$, where C and T are fitted parameters. The inverse slope parameter for protons in Pb + Pb collisions increases substantially from the slope parameter found in S + S collisions. A large degree of nuclear stopping is also observed in Pb + Pb collisions and this is attributed to copious secondary rescattering. The momentum distributions for the three particle species is consistent with a thermal model that includes radial flow.

Two-particle correlations have also been measured for pions and kaons for A + A collisions. The pion radii determined in the longitudinal, transverse-out, and transverse-side directions are similar and increase with the size of the collision system. Radii determined from kaon correlations are systematically smaller than radii determined from pion correlations. This fact suggests that kaons are possibly emitted from a more central region of the collision. It is also important to note that because kaons have fewer resonances contributions than pions, the measured radius parameters are smaller.

5 Acknowldgements

We are appreciative to the staff of the CERN PS-SPS accelerator complex for their excellent work. We thank the technical staff at CERN and the collaborating institutes for their valuable contributions. We are grateful for the support given by the Austrian Fonds zur Foerderung der wissenschaftlichen Forschung; the Science Research Council of Denmark; the Japanese Society for the Promotion of Science, and the Ministry of Education, Science and Culture, Japan; the Science Research Council of Sweden; the US Department of Energy; and the National Science Foundation (Nuclear Physics).

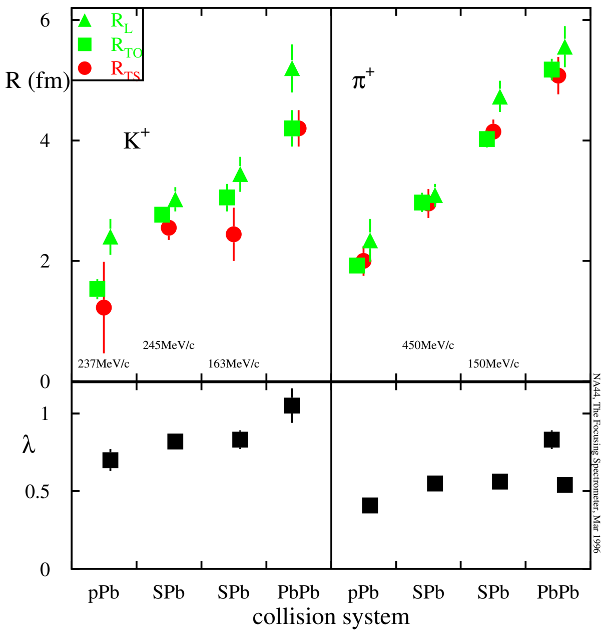

Figure 4: Summary of the radii and chaoticity parameters for A + A collisions for NA44. A comparision of the high and low momentum measurements is also shown for S + Pb data.

References

[1] C.W. Fabjan *et al.*,NIM A **367** (1995)240.

[2] H. Beker *et al.*, Phys. Lett. **B302**(1993)510.

[3] J. Bachler *el al.*, (NA35 Collaboration), Phys. Rev. Lett. **72**(1994)1419.

[4] H. Beker *et al.*,Z. Phys. **C64**(1994)209.

[5] L.D. Landau, *"Collected papers of Landau"*, Gordon and Breach, New York, 1965.

[6] E. Schnedermann, J. Sollfrank, and U. Heinz, Phys. Rev **C48**(1993)2462, and E. Schnedermann, J. Sollfrank, and U. Heinz, *"Particle Production in Highly Excited Matter"*,p. 175 E. H. Gutbrod and J. Rafelski, Plenum Press, New York 1992.

[7] H. Sorge *et al.*, Phys. Lett. **B289**(1992)6.

[8] B. Andersson *et al.*, Nucl. Phys. **B281**(1987)289.

[9] A. von Keitz *et al.*, Phys. Lett. **B263**(1991)353.

[10] P. Seyboth, Proceedings of XXXI Rencontres de Moriond (High Energy Hadronic Interactions), (1995).

[11] R. Hanbury-Brown and R.Q. Twiss, Nature (London) **178**(1956)1046.

[12] H. Beker *et al.*, Phys. Rev. Lett. **74**(1995)3340.

[13] S. Pratt, Phys. Rev. **D33**(1986)1314.

[14] G. Bertsch and G.E. Brown, Phys. Rev. **C40**(1989)1830.